J. Membrane Biol. 171, 171–176 (1999)

The Journal of
Membrane
Biology

Osmotic Equilibrium and Elastic Properties of Eel Intestinal Vesicles

P. Alves[1], G. Soveral[1,2], R.I. Macey[3], T.F. Moura[1]

[1]Dep. Química, Centro de Química Fina e Biotecnologia, Faculdade de Ciências e Tecnologia, Universidade Nova de Lisboa, Quinta da Torre, 2825 Monte da Caparica, Portugal

[2]Faculdade de Farmácia, Universidade de Lisboa, 1690 Lisboa, Portugal

[3]Department of Molecular and Cell Biology, University of California, Berkeley, CA 94720, USA

Received: 28 January 1999/Revised: 15 June 1999

Abstract. Changes in volume of intestinal brush border membrane vesicles of the European eel *Anguilla anguilla* were measured as vesicles were exposed to media with different osmotic pressures. Preparing the vesicles in media of low osmotic pressure allowed the effects of a small hydrostatic pressure to become a significant factor in the osmotic equilibration. By applying LaPlace's law to relate pressure and volume and assuming a linear relation between membrane tension and area expansion, we estimate an initial membrane tension at 4.02×10^{-5} N cm^{-1} and an area compressibility elastic modulus at 0.87×10^{-3} N cm^{-1}. The elastic modulus estimate falls in the low range of values reported for membranes from other tissues in other species. This lower modulus quantitatively accounts for why eel intestinal vesicles show measurable changes in volume in hypotonic media while rabbit kidney vesicles do not.

Key words: Eel intestinal vesicles — Elastic properties

Introduction

The migration of the European eel (*Anguilla anguilla*) between fresh and salt water presents osmotic challenges that are met by the combined actions of intestinal and gill epithelia. By drinking copious amounts of sea water, absorbing salt and water through the intestine and then excreting the salt through gills, the eel manages an uptake of water that is essential to balance other water losses into a hypertonic environment. Given this physiological function it would not be surprising to find the intestinal mucosa repeatedly challenged by osmotic as well as mechanical stress.

The coupling of membrane stress to transport and cell volume regulation via stretch-activated channels has been inferred in numerous systems (Miyamoto & Fujime, 1988; Miyamoto, Maeda & Fujime, 1988; Morris, 1990). In the case of eel intestine stretch-activated Na/K channels have been identified and characterized by Chang and Loretz (1992). These channels are activated by both strong membrane depolarization and the application of small hydrostatic pressures. Membrane tension generated by the applied pressure shifts the voltage dependence of channel activity into the physiological range. Chang and Loretz suggest that the channel may be part of a salt and water absorptive process or that it may be involved in cell volume regulation. In any case it is reasonable to clarify the connection between the osmotic behavior of intestinal cells and their elastic properties so that both applied pressures and osmotic stress can be translated into more pertinent membrane tension.

In conventional osmotic studies in animal cells it is common to disregard internal hydrostatic pressures because they are insignificant compared to osmotic forces. However, by using low osmolarities in small radii vesicles prepared from rabbit renal brush border, Soveral, Macey and Moura (1997*a*) were able to unmask evidence for an internal hydrostatic pressure that could be measured and utilized to assess elastic properties of the membrane. The pressure appears to be generated by osmotic contributions of internal nondiffusible solutes. Evidence for its existence included: (i) the nonlinear dependence of volume on the reciprocal tonicity, (ii) the dependence of the volume changes induced by the same tonicity shocks on the preparation buffer osmolarity, (iii) the influx of mannitol that follows an osmotic shock, and (iv) a Donnan ratio that departs significantly from unity.

Correspondence to: T.F. Moura

These diverse effects could be accounted for quantitatively if it were assumed that the vesicles contained impermeable solutes which, together with their counterions contributed around 18 mosM to the internal osmotic pressure. Further, by manipulating this pressure an elastic modulus as well as a membrane tension could be retrieved that fell within the range of literature values for red cells and liposomes.

In this paper we apply similar techniques (Soveral et al., 1997*a*) to relate the elastic and osmotic equilibria of brush border membrane vesicles isolated from the intestine of the European eel. In comparison to kidney vesicles, we find that eel vesicles have a lower elastic modulus which becomes apparent in the larger range of measurable volume changes in hypotonic media.

Materials and Methods

Preparation of Brush Border Membrane Vesicles

Eel intestine brush-border membrane vesicles (BBMV) were prepared by a two step-Mg^{2+} precipitation technique according to previously described techniques (Biber et al., 1981; Storelli, Vilella & Cassano, 1986). Briefly, eel (150–300 g) maintained at 4°C in controlled salinity (50% sea water) medium, were killed and the intestines were removed and washed in ice-cold isotonic buffered solution (154 mM NaCl, 2 mM Tris-Hepes pH 7.4). All steps were performed at 4°C. The intestines were homogenized in a Waring blender, low speed, 3 min, to obtain a ratio of 1 g of tissue to 10 ml buffer (300 mM mannitol, 12 mM Tris-EGTA pH 7.4), and then diluted with double distilled water (1:40 *w/v* ratio). A 1 M solution of $MgCl_2$ was added to this homogenate until a final concentration of 12 mM was reached. The mixture was stirred for 15 min and centrifuged at 2,500 × *g* for 15 min in a Beckman J2-21M/E refrigerated centrifuge. The supernatant was carefully removed and centrifuged at 39,000 × *g* for 30 min. The pellet was then homogenized with a glass teflon homogenizer (10 strokes at 1,000 rpm) in a buffer (1:12 *w/v* ratio) consisting of 60 mM mannitol, 6 mM EGTA-Tris pH 7.4. Once again a 1 M solution of $MgCl_2$ was added to this homogenate to reach the final concentration of 12 mM. The mixture was stirred for 15 min, centrifuged at 5,900 × *g* and the supernatant was carefully removed and centrifuged at 39,000 × *g* for 30 min. This step was repeated once, changing the ratio of pellet to transport study buffer to 1:10 *w/v*, and centrifuged at 39,000 × *g* for 30 min. The final brush border membrane vesicles were resuspended in an appropriate volume of buffer (cellobiose, 1 mM $MgCl_2$, 2 mM Tris-Hepes pH 7.4; final osmolarity 18 or 113 mosM). The membrane preparations were either used immediately or stored in liquid nitrogen for later use.

Renal brush border membrane vesicles were prepared from rabbit renal cortex according to previously described techniques (Soveral et al., 1997*a*) using a buffer containing 16 mM cellobiose, 2 mM Tris-Hepes pH 7.4 with final osmolarity 18 mosM.

Enrichment in specific activity (BBMV/crude homogenate ± SD) of the apical markers leucine-amino peptidase (Haase et al., 1978; Kramers & Robinson, 1979) and alkaline phosphatase (Berner & Kinne, 1976; Quamme, 1990) as well as the basolateral markers Na^+/K^+ ATPase (Quigley & Gotterer, 1969; Schoner et al, 1967) and K^+-stimulated phosphatase (Garrahan, Pouchan & Rega, 1969; Murer et al., 1976), assayed as described, were 16.7 ± 1.49, 9.4 ± 2.71, 0.55 ± 0.08 and 1.4 ± 0.09 ($n = 11$), respectively for intestinal eel vesicles and 16.6 ± 2.7, 8.6 ± 2.3, 1.3 ± 0.04 and 0.4 ± 0.09 ($n = 16$) for rabbit kidney vesicles.

Protein content was determined using the Bradford technique (Bradford, 1976) with bovine albumin as standard.

All solution osmolarities were determined from freezing point depression on a cryometric automatic semi-micro osmometer (Knauer GmbH, Germany). Standards of 20, 100 and 400 mosM were analyzed prior to samples, which were measured in triplicate.

Vesicle Size Determination

Vesicle size (initial equilibrium volume) of all the membrane preparations was determined by quasi-elastic light scatter (QELS) using a particle sizer (BI-90 Brookhaven Instruments) as already described (Soveral et al., 1997*a*).

The equilibrium volumes of renal proximal tubule vesicles subjected to several osmotic shocks with an impermeant solute, were achieved by vesicle trapped volume measurements using an isotope tracer (Soveral et al., 1997*a*).

Stopped Flow Experiments

Stopped flow experiments were performed on a HI-TECH Scientific PQ/SF-53 stopped-flow apparatus, which has a 2 msec dead time (mixing time less than dead time). Three runs were stored and analyzed in each experimental condition. In each run, 0.1 ml of vesicle suspension (0.4 mg protein/ml, in 18 or 113 mosM cellobiose buffer) was mixed with equal amounts of hypo- or hypertonic cellobiose buffer. The time course of 90° scattered light intensity at 400 nm was followed for different time intervals at a controlled temperature (23°C). In all experiments the photomultiplier voltage was adjusted to begin with the same constant value of scattered light intensity $I = I_o$ for the unperturbed vesicles.

Results

Osmotic Equilibrium — Calibration

Eel intestinal brush border vesicles prepared in 18 mosM cellobiose buffer, have a mean diameter ± SD of 324 ± 14 nm as measured by QELS, a value similar to the BBMV from rabbit kidney proximal tubule cells prepared in the same medium (347 ± 12 nm).

For rabbit kidney vesicles, the scattered light intensity signals were calibrated with independent volume measurements as described in (Soveral et al., 1997*a*). The same techniques could not be applied to eel vesicles because their volumes were not stable in an isotonic media over the long duration required for calibration measurement. Fortunately, their light-scattering properties were sufficiently similar to kidney vesicles to allow the use of the same calibration curve for both kidney and eel vesicles (*see* Eqs. (3), (6), and (7) below). This similarity can be seen in Fig. 1 which compares the change in light scatter intensity signal when eel intestine and rabbit kidney vesicles, equilibrated in their preparation buffer at osmolarity $(osm_{out})_o$, are suddenly transferred to the

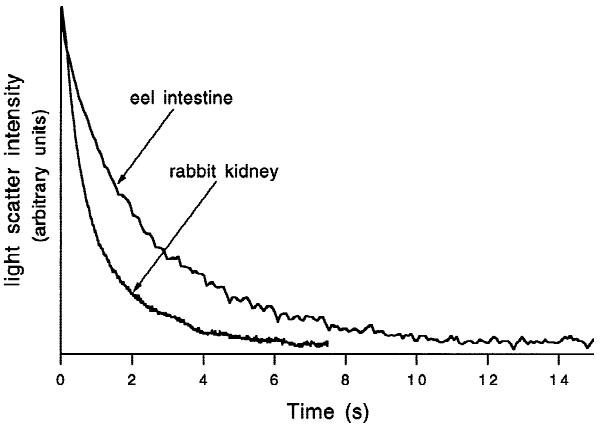

Fig. 1. Record of stopped-flow experiments where BBMV prepared from eel intestine and rabbit kidney in the same 18 mosM buffer were exposed to the same osmotic shock $\Lambda = (osm_{out})_\infty/(osm_{out})_o = 2.4$. The change in the light scatter intensity (I) was followed until the new osmotic equilibrium was reached.

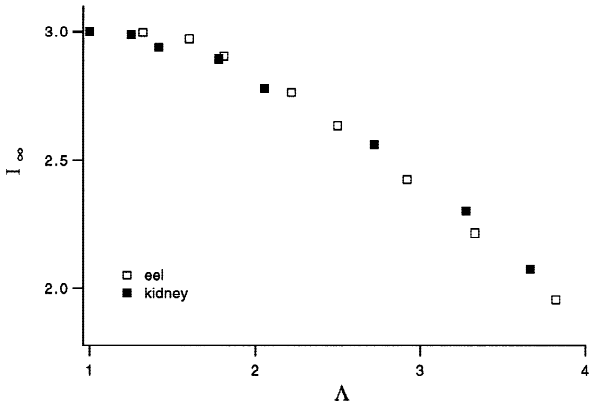

Fig. 2. Final light scatter intensity (I_∞) obtained from suspensions of eel intestinal or rabbit kidney vesicles subjected to different hyperosmotic shocks, in stopped flow experiments where the initial scatter intensity (I_o) was adjusted to a constant value.

same medium at osmolarity $(osm_{out})_\infty$. In this case the new medium is hypertonic and the vesicles shrink from an initial volume given by V_o to a new volume, V_∞. Although the vesicles shrink at different rates (reflecting differences in water permeability), both traces have the same total light scatter amplitude. This latter fact holds in general; Figure 2 shows that for the same osmotic shock Λ (Eq. (1)), the final light scatter intensity I_∞ of kidney and eel vesicles are indistinguishable if I_o is constant.

Justification for using the same calibration curve for both vesicles is given by the following: First, consider the conditions for equilibrium following an osmotic shock. Introducing dimensionless variables by using the initial volume V_o and initial medium osmolarity $(osm_{out})_o$ as normalizing factors, we define

$$\left.\begin{aligned} v &= V/V_o \\ \Lambda &= (osm_{out})_\infty/(osm_{out})_o \\ p &= \Delta P/(RT(osm_{out})_o) \end{aligned}\right\} \quad (1)$$

where ΔP is the hydrostatic pressure across the membrane and RT is the gas constant times the absolute temperature. Then a simple application of Van't Hoff's law (Soveral et al., 1997*a*) yields

$$\Lambda = \frac{1 + p_o}{v_\infty} - p_\infty \quad (2)$$

where p_o represents the initial p, and p_∞ and v_∞ represent the final equilibrium values of p and v. Hydrostatic pressure within the vesicles arises when there are nondiffusible internal solutes that are not balanced by the osmolarity in the external medium. When the vesicles are exposed to a hypertonic shock, they shrink and the internal pressure decreases, tending to zero as the tonicity rises. Equation (2) predicts that when the pressure becomes insignificant (i.e., for small volumes where $p_\infty = 0$), a plot of Λ *vs.* $1/v_\infty$ yields a straight line with an extrapolated intercept at the origin. Further, the slope of this line is, according to Eq. (1), a linear function of $1/(osm_{out})_o$. Equation (2) has been verified for kidney vesicles in detail (Soveral et al., 1997*a*); the straight line plot of Λ *vs.* $1/v_\infty$ became apparent at volumes less than a critical volume $v_\infty^* = 0.96$ (where $p_\infty = 0$) while the straight line plot of the *slope vs.* $1/(osm_{out})_o$ yielded a value for $\Delta P_o/RT \approx 18$ mosM.

Now consider the calibration. In Soveral, Macey and Moura (1997*b*), the volume of kidney vesicles was shown to be a linear function of $1/I$, i.e.,

$$(v_k)_\infty = (1 - b_k)\frac{I_{ko}}{I_k} + b_k \qquad \text{for } v < v_\infty^* \quad (3)$$

where I_{ko} and b_k are constants which define the linear relation and the subscript k refers to kidney vesicles. Note that I_{ko} is simply the light scattering signal of the unperturbed vesicle; i.e., when $(v_k)_\infty = 1$, $I_k = I_{ko}$. From Eq. (2), when $p_\infty = 0$, we also have $(v_k)_\infty = (1 + p_{ko})/\Lambda$. Combining this with Eq. (3) gives

$$\frac{1}{\Lambda} = \frac{(1 - b_k)}{(1 + p_{ko})}\frac{I_{ko}}{I_k} + \frac{b_k}{(1 + p_{ko})} \quad (4)$$

Applying the same arguments to eel vesicles we have

$$\frac{1}{\Lambda} = \frac{(1 - b_e)}{(1 + p_{eo})}\frac{I_{eo}}{I_e} + \frac{b_e}{(1 + p_{eo})} \quad (5)$$

where the subscript e now refers to eel vesicles and the constants b_e and I_{eo} define the calibration curve for the

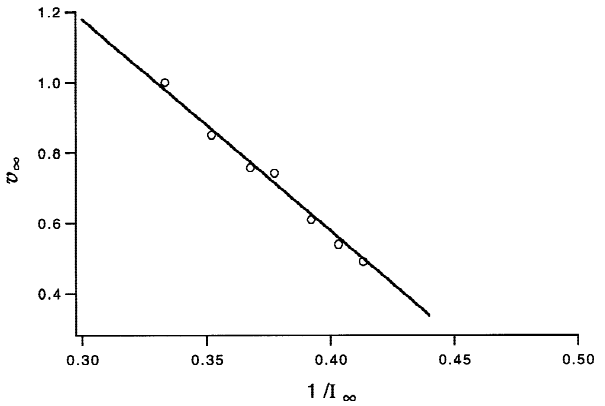

Fig. 3. Change of final vesicular volume (v_∞) as a function of the reciprocal final light scatter intensity ($1/I_\infty$) obtained when BBMV were subjected to different osmotic shocks in a stopped flow apparatus.

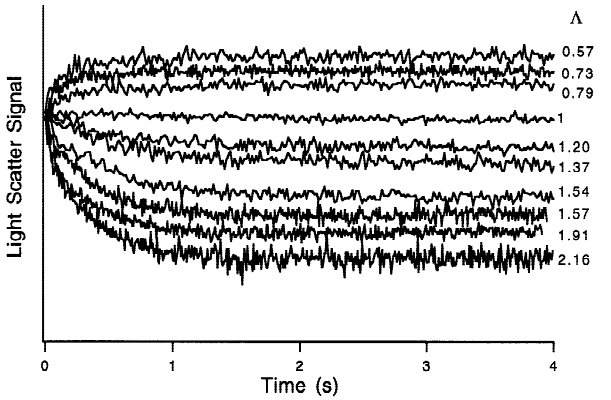

Fig. 4. Record of stopped flow experiments where the light scatter intensity $I(t)$ from a vesicle suspension prepared in 113 mosM cellobiose buffer was exposed to different osmotic shocks (Λ).

volume of eel vesicles (a linear function of $1/I_e$). In all experiments (both eel and kidney vesicles) the photomultiplier voltage is adjusted to arrive at the same constant value, $I = I_o$, for the unperturbed vesicles, i.e., we set $I_{eo} = I_{ko} = I_o$. Further the results of I_∞ *vs.* Λ in Fig. 2 show that for any given Λ over its entire range, the light scattering signals of eel and kidney vesicles are indistinguishable; i.e., $I_e = I_k = I$. Using these equalities and equating the right hand sides of Eqs. (4) and (5) leaves

$$\frac{(1-b_e)}{(1+p_{eo})}\frac{I_o}{I}+\frac{b_e}{(1+p_{eo})}=\frac{(1-b_k)}{(1+p_{ko})}\frac{I_o}{I}+\frac{b_k}{(1+p_{ko})} \tag{6}$$

But, these two linear functions of $1/I$ will be equal if and only if their coefficients are equal, i.e.,

$$\frac{b_e}{(1+p_{eo})}=\frac{b_k}{(1+p_{ko})}, \qquad \frac{(1-b_e)}{(1+p_{eo})}=\frac{(1-b_k)}{(1+p_{ko})} \tag{7}$$

It follows that $b_e = b_k$, $p_{eo} = p_{ko}$, and the same calibration applies to both vesicles. It also follows from Eq. (1) that $\Delta P_{eo} = \Delta P_{ko}$.

The final equilibrium volume v_∞ for the 18 mosM eel vesicles were taken directly from the kidney data since both vesicles were prepared in the same medium. For the 113 mosM eel vesicles, volumes were obtained by use of the linear portion (i.e., for $\Lambda \geq 1.2$) of Eq. (2) where $v_\infty = (1 + p_{eo})/\Lambda$. The value of p_{eo} (= 1.16 for 113 mosM vesicles) was calculated using the above value of $\Delta P_o/RT$ = 18 mosM.

Figure 3 shows a plot of v_∞ *vs.* $1/I_\infty$ for 113 mosM vesicles (mean diameter 320 ± 10 nm). The data points were restricted to osmotic shocks with $\Lambda \geq 1.2$ except for the isotonic data point. For each equilibrium volume the corresponding $1/I_\infty$ (taken from Fig. 4) was plotted and a straight line was fit to the data. This line was extrapolated for $v_\infty > 1$, in order to obtain the final equilibrium volumes for osmotic shocks with $\Lambda < 1$ as shown.

Elastic Properties

The membrane tension σ created by ΔP is governed by Laplace's law. Letting r denote the vesicle radius

$$\sigma=\frac{\Delta P r}{2}=\frac{RT(osm_{out})_o}{2}\left[\Lambda-\left(\frac{1+p_o}{v}\right)\right]r \tag{8}$$

where the last equality is obtained by use of Eqs. (1) and (2). Assuming the vesicles maintain a spherical shape for all $p_\infty > 0$, all quantities on the right hand side are measurable so that σ corresponding to each v_∞ (or r_∞) can be calculated from the experiments described above.

On the other hand, assuming a linear relation between membrane tension and area expansion ΔA for small Δr (Evans, Waugh & Melnik, 1976) we have

$$\sigma=k\frac{\Delta A}{A}=k\frac{2\Delta r}{r}=2k\frac{r-r_{min}}{r_{min}}$$
$$=\left(2k\frac{r_o}{r_{min}}\right)\frac{r}{r_o}-2k \tag{9}$$

where r_{min} is the radius where ΔP and σ vanish and k is the area compressibility elastic modulus (N cm^{-1}). Thus, for $p_\infty > 0$, the plot of σ *vs.* r_∞ should yield a straight line where k can be determined from the slope and intercept.

Figure 5 shows the results when σ is obtained from experimental data via Eq. (8). Note that both sets of data (18 and 113 mosM) were used in the plot. All the data points resolve into a single plot as required by theory. The value of k is 0.87×10^{-3} N cm^{-1} while the initial membrane tension $\sigma_o = 4.02 \times 10^{-5}$ N cm^{-1}.

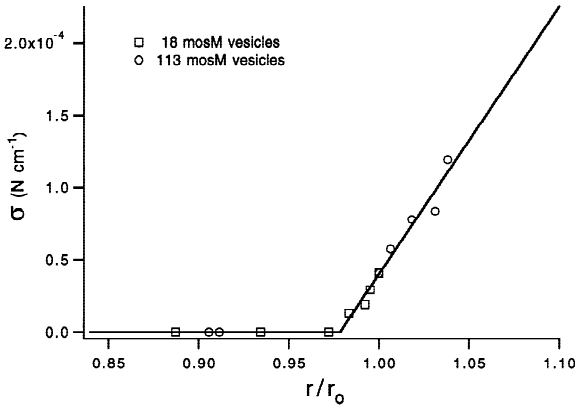

Fig. 5. Change of membrane tension (σ) as a function of vesicular radius (r/r_o). The data were rearranged according to Eq. (8) and were fit to Eq. (9) for $r > r_{min}$. The estimated values were $k = 0.87 \times 10^{-3}$ N cm^{-1} and $r_{min} = 0.98$ (corresponding to a critical volume $v_\infty^* = 0.94$, which compares well with the value 0.96 found for kidney vesicles).

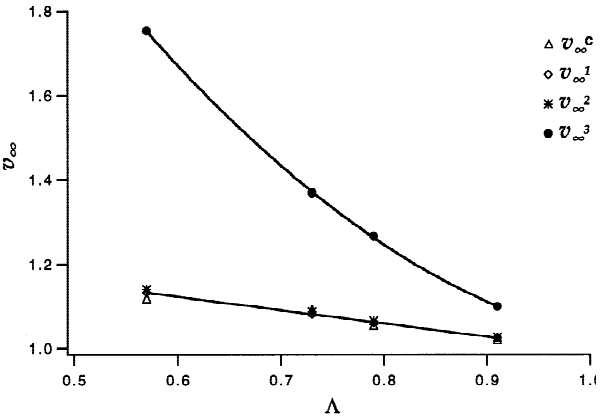

Fig. 6. Equilibrium volumes for different hypotonic shocks calculated with different methods. v_∞^c are the equilibrium volumes (for the hypotonic shocks of Fig. 4) calculated from the fit of Eq. (3) to data points in Fig. 3. v_∞^1 and v_∞^2 were calculated by Eqs. (2), (8) and (9) using the estimated k values (0.87 and 0.81×10^{-3} N cm^{-1}, respectively). v_∞^3 was calculated from Eq. (2) with $p_o = p_\infty = 0$.

Discussion

In our studies with kidney vesicles, we were not able to detect any volume change when the vesicles were exposed to hypotonic solutions (Soveral et al., 1997*a*). Presumably the p builds up very quickly to compensate for the osmotic imbalance before any appreciable volume change takes place. In contrast, the eel vesicles showed small, but measurable volume increases in hypotonic media. This reflects the lower k found in eels which dictates a larger volume increase for the same increment in pressure.

The fact that volume increases could be detected with eel vesicles prompted us to include the 113 mosM vesicles in this study so that data could be obtained with larger osmotic gradients. However, the use of strong hypo-osmotic gradients raises the issue of whether the vesicles leak solute in hypotonic media, and whether this leakage, rather than the buildup of p, was responsible for the very small volume change seen in hypotonic media. We do not believe that this is the case for the following reasons:

1. Hypertonic data, where no solute leakage occurs, can be used to predict the volume response to hypotonic shocks by assuming no leakage in the hypotonic media. If the hypotonic data are omitted from the plot of Fig. 5, the value of k changes very little (from 0.87×10^{-3} to 0.81×10^{-3}). Using these values of k, the volume change in hypotonic media, $v_\infty^{1,2}$, can be readily predicted from Eqs. (2), (8) and (9). The results illustrated in Fig. 6 show good agreement between the predicted ($v_\infty^{1,2}$) and measured (v_∞^c) volumes (from calibration), in contrast with the values calculated from Eq. (2) considering $p_o = p_\infty = 0$ (v_∞^3).

2. The kinetics of swelling in hypotonic media show no evidence of solute leakage. Volume changes were assessed with stopped flow light scattering which allows the final volume to be measured within 10 sec of the osmotic shock. Examination of the hypotonic swelling curves (Fig. 4), shows that within this time period the asymptotes are flat. If leakage of any consequence was occurring during this time we would expect to see the asymptotes returning toward the original volume. There is also no evidence of leakage during the transient which, when analyzed, yields an osmotic permeability constant that agrees with the permeability constant obtained from hypertonic shock data (Alves et al., 1999).

Our estimate for $k = 0.87 \times 10^{-3}$ N cm^{-1} from equilibrium data agrees with an independent estimate $k = 0.79 \times 10^{-3}$ N cm^{-1} obtained by analysis of osmotic transients (Alves et al., 1999). These figures fall in the low range of values reported for membranes from other tissues in other species. In red blood cells values range from 0.95×10^{-3} to 5.6×10^{-3} N cm^{-1} (Evans et al., 1976; Waugh & Evans, 1979; Hochmuth & Waugh, 1987). In liposomes, three laboratories report values from 3.4×10^{-3} to 6.3×10^{-3} N cm^{-1} (Hantz et al., 1986; Rutkowski et al., 1991; Hallett et al., 1993), although one laboratory finds that k ranges from 0.15 to 2×10^{-3} N cm^{-1} (Li et al., 1986). In brush border vesicles Miyamoto et al. (1988) estimate values for rat intestine ranging from 1.6 to 8×10^{-3} N cm^{-1}, and Soveral et al. (1997*a*) find $k = 2.8 \times 10^{-3}$ N cm^{-1} for renal brush border vesicles.

The apparently low value of the basic membrane elastic modulus in eel intestine may be relevant to the interpretation of stretch-activated channels. For example, the threshold pressure required to activate Na/K channels in eel intestine is lower than the threshold found

for similar channels in the urinary bladder (Chang & Loretz, 1992). This would be anticipated if the elastic modulus of intestine is also lower than in the urinary bladder. This can be seen by the following argument:

It is reasonable to assume that rather than ΔP, the more fundamental variable is membrane stress and that a stress threshold will be reached when σ reaches a critical value given by $\sigma = \sigma^*$. The dependence of corresponding pressure threshold ΔP^* on σ^* can be found by solving Eq. (8) for r, substituting the result into Eq. (9) and then solving Eq. (9) for ΔP, i.e.,

$$\Delta P^* = \frac{\frac{2\sigma^*}{r_{min}} k}{\frac{\sigma^*}{2} + k} \tag{10}$$

Equation (10) is a monotonic increasing function of k. Hence, given the same protein channel (with the same σ^*), the membrane with the lower k will have the lower threshold (provided that the local radius of curvature of the membrane is the same).

We thank the Fundação para a Ciência e Tecnologia for financial support to Prof. R.I. Macey who is a Visiting Professor at CQFB. This work was supported by grant PRAXIS XXI No 2/2.1/BIO/1159/95, and a fellowship Ciência BD/2524/93-RM to Paula Alves.

References

Alves, P., Soveral, G., Macey, R.I., Moura, T.F. 1999. Kinetics of water transport in eel intestinal vesicles. *J. Membrane Biol.* **171:**177–182

Berner, W., Kinne, R. 1976. Transport of p-aminohippuric acid by plasma membrane vesicles isolated from rat kidney cortex. *Pfuegers Arch.* **361:**269–277

Biber, J., Stieger, B., Haase, W., Murer, H. 1981. A high yield preparation for rat kidney brush border membranes. Different behaviour of lysosomal markers. *Biochim. Biophys. Acta* **647:**169–176

Bradford, M. 1976. A rapid and sensitive method for the quantitation of microgram quantities of protein utilizing the principle of protein-dye binding. *Anal. Biochem.* **72:**248–254

Chang, W., Loretz, C.A. 1992. Activation by membrane stretch and depolarization of an epithelial monovalent cation channel from teleost intestine. *J. Exp. Biol.* **169:**87–104

Evans, E.A., Waugh, R., Melnik, L. 1976. Elastic area compressibility modulus of red cell membrane. *Biophys. J.* **16:**585–595

Garrahan, P.J., Pouchan, M.I., Rega, A.F. 1969. Potassium-activated phosphatase from human red blood cells. The mechanism of potassium activation. *J. Physiol.* **202:**305–327

Haase, W., Schafer, A., Murer, H., Kinne, R. 1978. Studies on the orientation of brush border membrane vesicles. *Biochem. J.* **172:**57–62

Hallett, F.R., Marsh, J., Nickel, B.G., Wood, J.M. 1993. Mechanical properties of vesicles. II. A model for osmotic swelling and lysis. *Biophys. J.* **64:**435–442

Hantz, E., Cao, A., Escaig, J., Taillandier, E. 1986. The osmotic response of large unilamellar vesicles studied by quasielastic light scattering. *Biochim. Biophys. Acta* **862:**379–386

Hochmuth, R.M., Waugh, R.E. 1987. Erythrocyte membrane elasticity and viscosity. *Ann. Rev. Physiol.* **49:**209–219

Kramers, M.T.C., Robinson, G.B. 1979. Studies on the structure of the rabbit kidney brush border. *Eur. J. Biochem.* **99:**345–351

Li, W., Aurora, T.S., Haines, T.H., Cummins, H.Z. 1986. Elasticity of synthetic phospholipid vesicles and submitochondrial particles during osmotic swelling. *Biochemistry* **25:**8220–8229

Miyamoto, S., Fujime, S. 1988. Regulation by Ca^{2+} of membrane elasticity of bovine chromaffin granules. *FEBS Lett.* **238:**67–70

Miyamoto, S., Maeda, T., Fujime, S. 1988. Change in membrane elastic modulus on activation of glucose transport system of brush border membrane vesicles studied by osmotic swelling and dynamic light scattering. *Biophys. J.* **53:**505–512

Morris, C.E. 1990. Mechanosensitive ion channels. *J. Membrane Biol.* **113:**93–107

Murer, H., Ammann, E., Biber, J., Hopfer, U. 1976. The surface membrane of the small intestinal epithelial cell. 1. Localization of adenil cyclase. *Biochim. Biophys. Acta* **433:**509–519

Quamme, G.A. 1990. Effect of parathyroid hormone and dietary phosphate on phosphate transport in renal outer cortical and outer medullary brush-border membrane vesicles. *Biochim. Biophys. Acta* **1024:**122–130

Quigley, J.P., Gotterer, G.S. 1969. Distribution of (Na^+-K^+)-stimulated ATPase activity in rat intestinal mucosa. *Biochim. Biophys. Acta* **173:**456–468

Rutkowski, C.A., Williams, L.M., Haines, T.H., Cummins, H.Z. 1991. The elasticity of synthetic phospholipid vesicles obtained by photon correlation spectroscopy. *Biochemistry* **30:**5688–5696

Schoner, W., Ilberg, C., Kramer, R., Seubert, W. 1967. On the mechanism of Na^+- and K^+-stimulated hydrolysis of adenosine triphosphate. 1. Purification and properties of a Na^+- and K^+-activated ATPase from ox brain. *Eur. J. Biochem.* **1:**334–343

Soveral, G., Macey, R.I., Moura, T.F. 1997*a*. Mechanical properties of brush border membrane vesicles from kidney proximal tubule. *J. Membrane Biol.* **158:**209–217

Soveral, G., Macey, R.I., Moura, T.F. 1997*b*. Water permeability of brush border membrane vesicles from kidney proximal tubule. *J. Membrane Biol.* **158:**219–228

Storelli, C., Vilella, S., Cassano, G. 1986. Na-dependent D-glucose and L-alanine transport in eel intestinal brush border membrane vesicles. *Am. J. Physiol.* **251:**R463–R469

Waugh, R., Evans, E.A. 1979. Thermoelasticity of red blood cell membrane. *Biophys. J.* **26:**115–132